

# EEG and EMG Signal Analysis for the Early Detection of Parkinson's Disease

**Subhashini Gopal Krishnan**

School of Engineering, Asia Pacific University of Technology and Innovation, TPM, Kuala Lumpur, Malaysia  
subhashini@apu.edu.my

**Sathish Kumar Selva Perumal**

School of Engineering, Asia Pacific University of Technology and Innovation, TPM, Kuala Lumpur, Malaysia  
sathish@apu.edu.my (corresponding author)

**Kalaiselvi Aramugam**

School of Engineering, Asia Pacific University of Technology and Innovation, TPM, Kuala Lumpur, Malaysia  
kalaiselvi@apu.edu.my

**Mukil Alagirisamy**

School of Engineering, Asia Pacific University of Technology and Innovation, TPM, Kuala Lumpur, Malaysia  
mukil.alagirisamy@apu.edu.my

**Waweru Njeri**

Department of Electrical and Electronic Engineering, Dedan Kimathi University of Technology, Nyeri, Kenya  
waweru.njeri@dkut.ac.ke

**Victor Enrique Chiroque Landayeta**

Pontificia Universidad Catolica del Peru, Lima, Peru  
echiroq@pucep.edu.pe

**Helal Ahmed Helal**

Mechatronic Engineering Department, Asia Pacific University of Technology and Innovation, TPM, Kuala Lumpur, Malaysia  
helal.ahmed00@outlook.com

*Received: 29 December 2025 | Revised: 19 January 2026 and 3 February 2026 | Accepted: 4 February 2026*

*Licensed under a CC-BY 4.0 license | Copyright (c) by the authors | DOI: <https://doi.org/10.48084/etasr.17231>*

## ABSTRACT

Parkinson's Disease (PD) is a progressive neurodegenerative disorder that significantly impacts motor and cognitive function. Early and accurate diagnosis is a significant clinical challenge. This study proposes a hybrid deep learning framework that integrates Electroencephalography (EEG) and Electromyography (EMG) signals to classify PD patients. EEG signals were collected using the Emotiv Epoc X headset (14 channels, 10–20 system). At the same time, EMG data were acquired from three sensors placed according to the SENIAM standard (biceps, flexor carpi, extensor digitorum). Publicly available datasets, including the San Diego PD EEG dataset, were employed for model training and evaluation. Preprocessing included 1–50 Hz band pass filtering, Independent Component Analysis (ICA) for artifact removal, and epoch segmentation for EEG, while EMG signals underwent 20–450 Hz filtering, rectification, and RMS

smoothing. A hybrid Convolutional Neural Network (CNN)- Long Short-Term Memory (LSTM) architecture was developed in Python to capture spatial and temporal dependencies in the multimodal bio signals. The model achieved 99% classification accuracy with a training loss of 0.14, demonstrating strong predictive power for early-stage PD detection. Despite promising results, the study is limited by the use of only 14 EEG electrodes and three EMG electrodes, with recordings restricted to rest conditions. Future work will expand electrode coverage, incorporate additional limb-based EMG sensors, and evaluate PD-related neural and muscular activity during more diverse tasks, such as puzzle solving, handwriting, and typing. This research highlights the potential of multimodal deep learning approaches for early and non-invasive PD diagnosis.

**Keywords-EEG; EMG; PD; CNN; LSTM; Emotiv Epoc X**

## I. INTRODUCTION

Neurological and neuromuscular disorders progressively impair motor and cognitive functions, making early diagnosis critical for effective clinical intervention. Conventional diagnostic approaches often lack sensitivity to early-stage abnormalities, motivating the use of data-driven analysis of biomedical signals as a non-invasive alternative [1]. Electroencephalography (EEG) and Electromyography (EMG) are widely used to capture neural and muscular activity associated with neurological disorders. EMG-based machine learning methods have proven effective in detecting Parkinson's Disease (PD) and neuromuscular abnormalities through muscle activation patterns [2, 3], while EEG-based approaches successfully identify disease-related cortical changes [4]. Deep learning models have enhanced EEG-based diagnosis by enabling automatic feature learning and improved classification performance across neurological conditions [5, 6]. However, most existing studies rely on unimodal data, limiting their ability to capture the coupled neural-muscular manifestations of the disease. Multimodal analysis combining EEG and EMG offers a more comprehensive representation of motor dysfunction, provided that ethical data acquisition practices are followed [7, 8]. Nevertheless, challenges related to signal noise, feature robustness, and generalization remain [9, 10]. Addressing these gaps, the present study proposes a hybrid deep learning framework that integrates EEG and EMG signals for early and reliable neurological disorder detection. Recent advances also emphasize the importance of ethical and responsible artificial intelligence in biomedical applications, particularly when dealing with sensitive neurological data and automated decision-making systems [11]. From a methodological perspective, machine learning techniques have been successfully applied to classify EMG patterns in gait and neuromuscular disorders, demonstrating reliable discrimination capabilities [12, 13]. Further improvements have been achieved through multimodal fusion strategies that combine EEG and EMG signals, enabling more accurate representation of motor intent and dysfunction [14]. EEG-based machine learning models have shown strong potential for PD detection using resting-state recordings, including multi-center validations that highlight robustness across datasets [15, 16].

Deep learning architectures, particularly Convolutional Neural Network (CNN)-Long Short-Term Memory (LSTM) models, have further enhanced classification performance by capturing both spatial and temporal neural dynamics [17], while recent attention-based models have demonstrated effectiveness in identifying complex motor symptoms such as freezing of gait [18]. Research confirms the growing role of

artificial intelligence in automated neurological disorder detection using EEG signals [19]. Finally, biomedical signal acquisition and analysis must comply with established ethical principles for human-subject research and data protection regulations to ensure patient safety, privacy, and responsible deployment of intelligent diagnostic systems [20, 21].

## II. LITERATURE REVIEW

EMG-based diagnostic systems have been extensively studied for the detection of neuromuscular disorders, demonstrating reliable performance in identifying abnormal muscle activation patterns [2]. EMG signals have also been applied to PD diagnosis, where muscle tremors and rigidity-related features serve as key indicators [5]. In contrast, EEG-based diagnostic systems have primarily focused on neurological disorders, such as Amyotrophic Lateral Sclerosis (ALS), PD, and Autism Spectrum Disorder (ASD), by analyzing alterations in brain activity [4]. The combination of EEG and EMG signals has been explored to improve motor activity classification by capturing both neural and muscular information [8]. Machine learning techniques, particularly Support Vector Machines (SVM), have been widely adopted in these studies due to their robustness when dealing with limited datasets [9]. Despite promising diagnostic performance, many studies suffer from limitations related to small dataset sizes, which restrict model generalizability and clinical applicability [10]. Additionally, several works lack detailed reporting of dataset characteristics and validation procedures, making result reproducibility challenging [11]. Most existing diagnostic systems also rely on binary classification schemes, which limit their effectiveness in monitoring disease progression across multiple severity stages [12].

Deep learning approaches, especially CNNs, have been introduced for EEG-based neurological disorder diagnosis, achieving improved classification accuracy by automatically learning hierarchical feature representations [13]. However, these methods often require large datasets and high computational resources, which are challenging in clinical environments [14]. Previous studies focusing exclusively on EMG-based PD classification have shown that while muscle activity provides valuable diagnostic information, it fails to capture neural dysfunctions associated with disease progression [5]. Conversely, EEG-only approaches overlook muscular abnormalities, resulting in incomplete disease representation [4]. These findings highlight the necessity of developing integrated and scalable diagnostic frameworks that can support multi-class classification and long-term disease monitoring [12].

### III. METHODOLOGY

The current study begins with data acquisition, obtaining EEG and EMG signals from publicly available databases [15-21], while the EEG signal data are collected from the San Diego dataset [24] and UNM EEG dataset [25]. These datasets capture resting-state brain activity of Parkinsonian and normal subjects. EMG signals, if not from an available database, are assumed to be simulated or taken using cheap sensors such as the Muscle Sensor v3.0. After collection, signals are first preprocessed for the removal of noise and artifacts. The EEG signals are filtered with bandpass filters to retain components within the frequency ranges of interest (usually 0.5–50 Hz), and then Independent Component Analysis (ICA) is applied to remove ocular and muscular artifacts. EMG signals are filtered with the combination of high-pass and low-pass filters to discard motion artifacts and electrical noise, followed by rectification and smoothing to highlight the muscle activity.

Following preprocessing, the cleaned signal proceeds for feature generation, where segmentation into fixed-length windows and normalization are performed. Depending on the requirements of the model, these signals can be used in their raw time-series form or by converting each of them into time-frequency representations, such as the spectrogram or wavelet coefficients, to make the data compatible with the neural network model. The data are then forwarded to the hybrid CNN-LSTM model. CNN layers extract local spatial patterns in the EEG and EMG data by finding meaningful features in the signals. These features are then transmitted to the LSTM layers to learn temporal dependencies in the signals and detect the sequential patterns that may be indicative of PD. The model is trained in a supervised manner on labeled data from the database and produces a binary classification output. In the end, the classification output block displays the result indicating the presence of PD, given the input signals. This system provides an early-stage diagnosis in real-time, which makes use of biosignal data to support clinical decision-making. Figure 1 illustrates the workflow of the proposed EEG–EMG–based PD detection system.

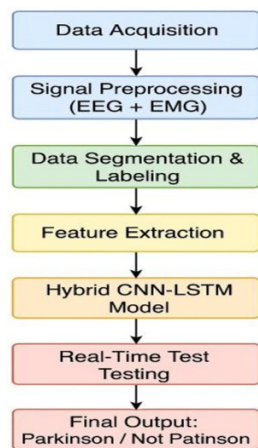


Fig. 1. Workflow of the proposed EEG–EMG–based PD detection system.

#### A. Electrode Placement

The electrodes are placed according to the 10–20 system on certain scalp regions, as shown in Figure 2. These regions are frequently correlated with motor and cognitive activity associated with Parkinson's pathology. The Emotiv Epoc X covers 14 EEG channels placed according to the international 10–20 system, focusing mainly on the frontal, temporal, parietal, and occipital lobes. The only areas that Emotiv Epoc X does not cover are Cz, CPz, and Pz. While these areas are important for research, the detection of PD is still possible without them. Table I summarizes the coverage of the Emotiv Epoc X sensor.

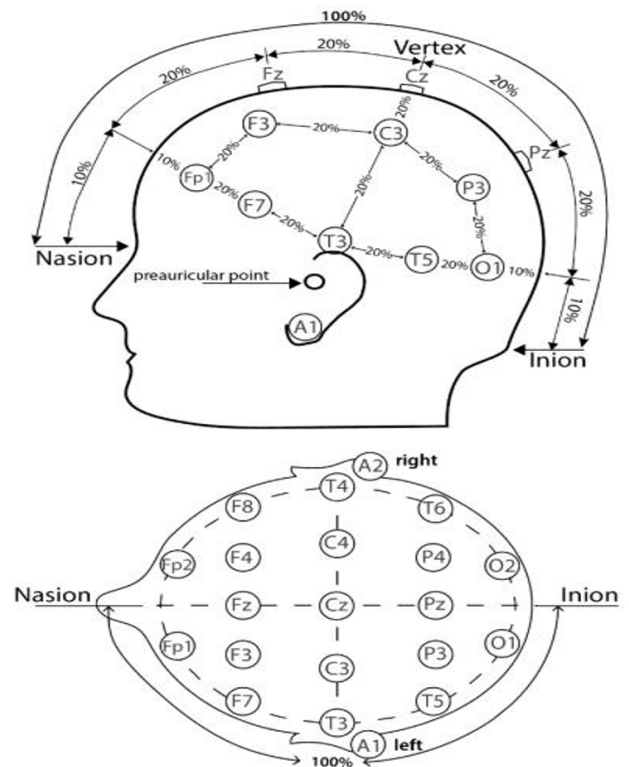


Fig. 2. Electrode placement on the 10–20 international system.

TABLE I. EMOTIV EPOC X 10–20 SYSTEM COVERAGE

Electrode name	10–20 system location	Brain area
AF3	Anterior frontal (left)	Prefrontal cortex (left)
F7	Frontal (left)	Frontal lobe (Broca's area)
F3	Frontal (left)	Frontal cortex
FC5	Fronto-central (left)	Motor cortex (left)
T7	Temporal (left)	Auditory cortex (left)
P7	Parietal (left)	Somatosensory (left)
O1	Occipital (left)	Visual cortex (left)
O2	Occipital (right)	Visual cortex (right)
P8	Parietal (right)	Somatosensory (right)
T8	Temporal (right)	Auditory cortex (right)
FC6	Fronto-central (right)	Motor cortex (right)
F4	Frontal (right)	Frontal cortex
F8	Frontal (right)	Frontal lobe
AF4	Anterior frontal (right)	Prefrontal cortex (right)

### B. EMG Electrode Placement

This study complies with the SENIAM protocol for surface EMG electrode placement, as detailed in [7], which outlines the identification of 12 sites anatomically consistent with the muscle to ensure the integrity and reproducibility of the EMG signal. Figure 3 displays the EMG electrode placements based on SENIAM guidelines. As this study focuses on PD detection, only three areas are considered, which are solid in detecting muscle weakness and tremor. These are E1: the biceps brachii lateralis (2), E2: the flexor carpi radialis (10), and E3: the extensor digitorum (5). The biceps brachii lateralis, being an important upper arm flexor and rigidity detector, is usually affected in PD patients. The flexor carpi radialis is chosen in order to study fine motor control and bradykinesia, being responsible for wrist flexion. The extensor digitorum, which extends the fingers, helps understand tremor patterns and the precision of voluntary movements.

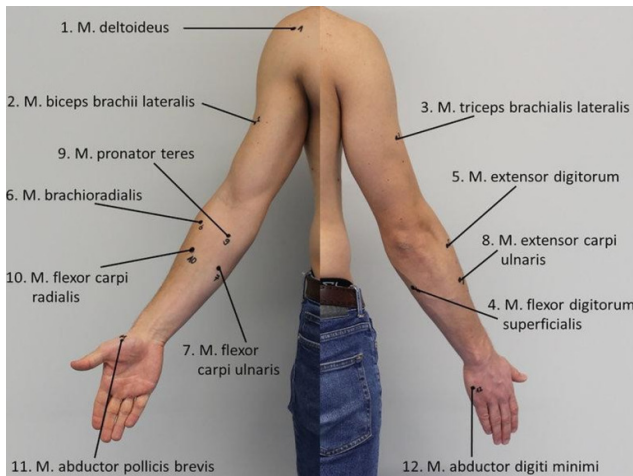


Fig. 3. EMG electrode placements based on SENIAM guidelines. © by authors in [7] under CC 4.0.

### C. Machine Learning and Prediction Model

For the classification of PD using biosignals (EEG and EMG), this study utilizes a hybrid machine learning model based on CNN and LSTM systems. Feature extraction is carried out by the CNN. Local patterns in time series EMG or EEG data, namely changes in frequency, amplitude, or noise features that mark Parkinsonian motor symptoms, are captured using convolutional filters. This process eliminates the manual feature engineering requirement and ensures that the spatial features, most useful for classification, are extracted from either raw or preprocessed signals. LSTMs are then employed to capture the temporal dependencies and sequential nature of the biosignals. Since such abnormalities, characteristic of Parkinson-like tremors or muscular rigidity, occur in time-dependent repeating patterns, LSTM stands out as an optimal choice as it can remember previous inputs in a time series and model longer-time dependencies. The CNN-LSTM hybrid model is capable of identifying subtle abnormalities in biomedical signals related to PD with superior pattern recognition in spatial terms through CNN and sequence learning in temporal terms through LSTM. This leads to higher accuracy, better generalization, and a structurally more robust

working environment in both training and real-time testing. Figure 4 presents the flowchart of the proposed method.

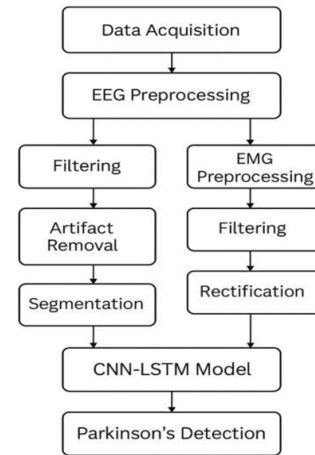


Fig. 4. Flowchart of the proposed method for PD detection using EMG and EEG signals.

## IV. IMPLEMENTATION

The EEG headset (Emotiv EPOC X) connects to the Raspberry Pi (microcomputer) wirelessly via Bluetooth, since it has a built-in battery and transmitter. Raspberry Pi wirelessly receives EEG data streams without ADC conversion. In contrast, the EMG sensor produces an analog voltage that cannot be processed directly by the microcomputer. To address this, the ADS1015 Analog-to-Digital Converter (ADC) is placed between the EMG sensor and the microcomputer. The ADC converts the continuous analog muscle signals into digital signals that the Raspberry Pi can process over the I<sup>2</sup>C bus, using GPIO2/SDA and GPIO3/SCL. For the EMG connection, the sensor's VCC is powered by the Pi's 3.3 V pin, GND is connected to the Pi's ground, and the sensor's signal output is transferred to one of the ADS1015's input channels (A0–A3). The ADS1015 is also powered by 3.3 V and shares the same ground. ADC communicates with the Raspberry Pi over I<sup>2</sup>C, providing digitized EMG samples that can be used alongside EEG data for PD detection experiments. The system works in two modes: prediction of recorded EEG and EMG data, and real-time prediction.

TABLE II. CONNECTION OF THE EMG SENSOR TO ADS1015 AND RASPBERRY PI

Component	Pin	Connects to	Notes
ADS1015	VDD	Pi 3.3 V (Pin 1)	Power supply (3.3 V)
	GND	Pi GND (Pin 9)	Common ground
	SDA	Pi GPIO2 (Pin 3)	I <sup>2</sup> C data
	SCL	Pi GPIO3 (Pin 5)	I <sup>2</sup> C clock
	ADDR	GND	Sets I <sup>2</sup> C address = 0x48
	A0	EMG sensor output	Signal input
EMG sensor	VCC	Pi 3.3 V	Power
	GND	Pi GND (Pin 9)	Ground
	OUT	ADS1015 A0	Analog signal line

### A. Prediction Based on Sample Files

In this mode, the system performs prediction using previously recorded EEG and EMG signals that are provided as

input files (e.g., CSV format). The system is designed to handle 14 EEG channels from the Emotiv Epoc X headset and 1 EMG channel from a muscle activity sensor, resulting in 15 synchronized input signals, as shown in Figure 5. Each signal is segmented into fixed-size windows of 1024 samples, ensuring a consistent input structure for the deep learning model. The motivation for this feature is to allow external users to record data independently—using compatible hardware setups—and then submit these files to the system for PD prediction. This is especially useful in cloud-based or remote diagnostic settings, where the system can be queried on demand by uploading a dataset. The minimum required recording length depends on the acquisition sampling rate. For example, with a sampling rate of 512 Hz, only 2 s of data are sufficient to fill one window of 1024 samples. At a lower sampling rate of 128 Hz, at least 8 s of data are required to form one window. Regardless of the

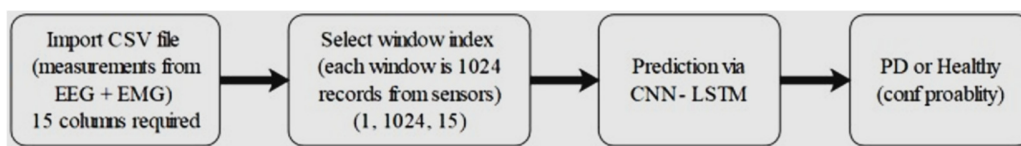


Fig. 5. Workflow of the prediction process based on sample files.

### B. Prediction in Real Time

This mode can work in real time and interact directly with the EEG and EMG sensors to analyze physiological signals in real time. Sampling can be done from 128 Hz to 512 Hz, depending on the hardware specification and user preference. As soon as these signals are captured, they are plotted in real time to demonstrate live feedback on the ongoing acquisition process, as exhibited in Figure 6. The incoming data are continuously buffered, and once a full buffer of 1024 samples is received, the prediction pipeline is triggered. These data are further processed through the CNN+LSTM model to yield the classification of either PD or healthy, along with their corresponding probability score. This information is then shown in a tabular interface, logging each window processed in the sample number, prediction outcome, and confidence level associated with it. Furthermore, both the raw data and the model-based prediction results are kept in a .dat file for future analysis and reference. The model, while trained specifically for resting-state activity, as was the case with the San Diego and NatMEG-PD datasets, requires users to stay in the rest condition (sitting still with minimum movements) while recording and predicting.

## V. RESULTS

The hybrid model based on CNN-LSTM effectively differentiates between the PD and healthy candidates based on the sample files in the dataset. The proposed CNN-LSTM model achieved an accuracy of 99.89% and a validation accuracy of 100%. There was no sign of over-fitting in the trained model, resulting from the comparison between two other developed models. The performance of the hyperparameter-tuned CNN-LSTM model (Model 3) is further illustrated through several visualizations. Table III and Figures 7 and 8 illustrate the accuracy and loss during training and validation, respectively.

recording length, the system splits the data into 1024-sample windows, each of which is independently fed into the prediction model.

The backend model combines CNN for feature extraction with LSTM networks for temporal sequence learning [22]. The model outputs a probability value in the range of 0–1:

- Values closer to 1 represent strong evidence of PD.
- Values closer to 0 are strong evidence of a healthy person.
- Values around 0.5 demonstrate weak confidence (e.g., 0.51 would suggest PD with low certainty, while 0.49 would suggest healthy with low certainty).

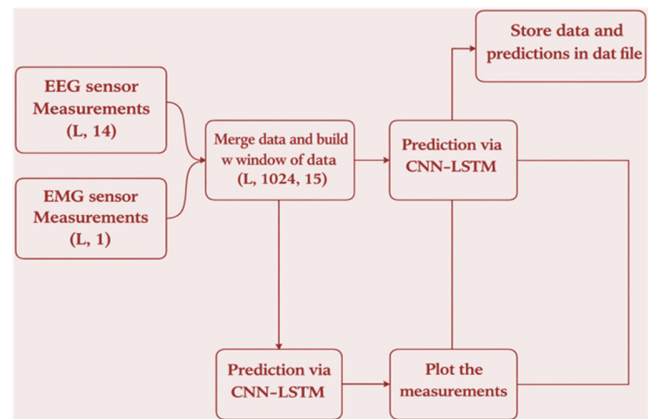


Fig. 6. Real-time prediction process.

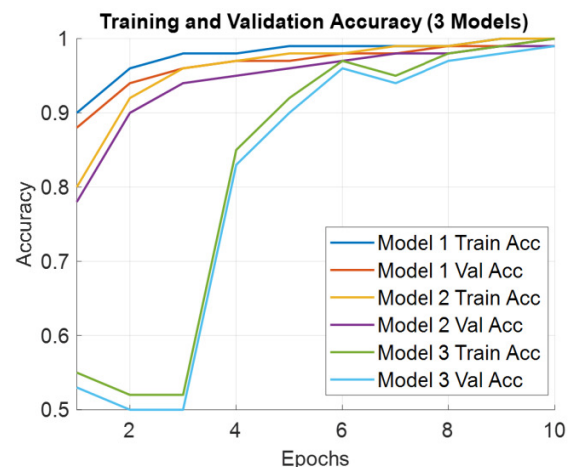


Fig. 7. Training and validation accuracy for three models.

Additionally, the confusion matrices, as depicted in Figures 9 and 10, illustrate the counts of true positives, false positives, true negatives, and false negatives for each class. The perfect diagonal of the matrix indicates that all 256 healthy and 240 PD samples were correctly classified, with no misclassifications. The normalized confusion matrix, shown in Figure 10, illustrates the relative values for every class in relative proportion to the total sample input. The normalized values 1.0 for both classes support the assumption of perfect performance by the model. The ROC curve, as displayed in Figure 11, is a binary classification function, in which true positive rates are plotted against false positive rates for different probability thresholds.

The ROC area of 1.0 shows a perfect separation between healthy and PD samples at the top left corner. It also demonstrates the precise classification capabilities of Model 3 for each class and good generalization abilities on new test data. In addition, Model 3 also demonstrates a perfect classification performance on the test set. For both the Healthy and PD classes, the precision, recall, and F1-score of 1.0 indicate that each sample was classified correctly in the test

data. Therefore, all 256 healthy and 240 PD samples were correctly predicted, resulting in a confusion matrix with a perfect diagonal and no misclassified samples.

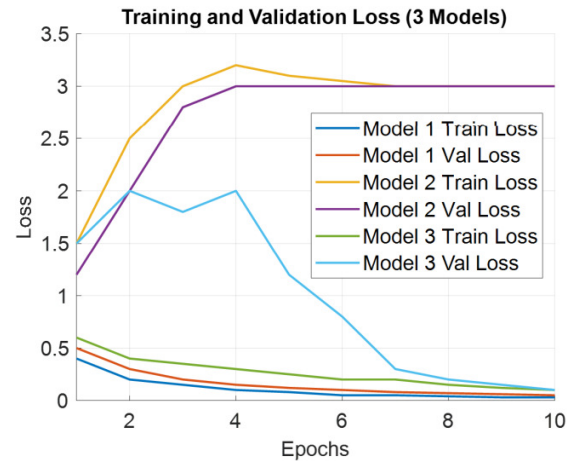


Fig. 8. Training and validation loss for three models.

TABLE III. TRAINING AND VALIDATION PERFORMANCE OF THREE MODELS

Model	Epochs	Training loss	Training accuracy	Validation loss	Validation accuracy
Model 1	5	0.000603	1.0000	3.2474	0.5000
Model 2	5	0.0239	0.9950	3.1366	0.5484
Model 3	11	0.1301	0.9989	0.1191	1.0000

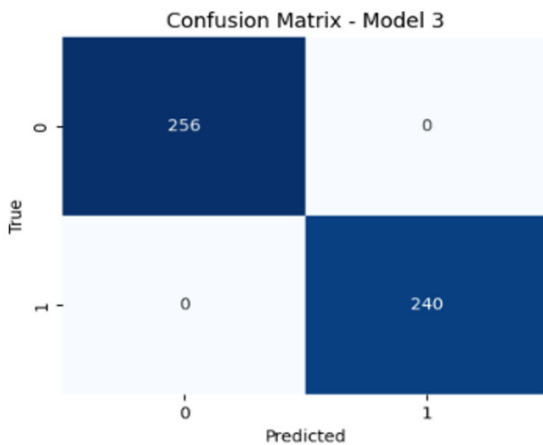


Fig. 9. Confusion matrix of Model 3.

Overall, the proposed model achieved an accuracy of 100% for macro average and weighted averages, indicating excellent performance across both classes without bias. This performance is further corroborated by a specificity score of 1 for both classes, indicating that true negatives and true positives were correctly identified by the proposed model. Furthermore, Figure 12 shows the learning curve of Model 3 for different training set sizes, indicating improved performance with an increase in training data. Similar limitations persist at full data usage, while the best performance is observed when 60%–80% of the training data is used.

The stability test evaluates whether the accuracy reported during training and validation occurred by chance or remained

consistent. This test simulates the model with a similar configuration over the same set of training data and validation subset for over 5 runs. The result indicates that the model in all 5 runs shows strong accuracy for both validation and training, with a low standard deviation of 0.0040. The training accuracy ranges from 0.9878 to 0.9994, as depicted in Figure 13, indicating that the model almost perfectly learns the training data. In contrast, the validation accuracy is considerably more variable (mean = 0.9298, std = 0.1248, range = 0.6815–1.0000), suggesting that generalization to unseen validation data is less stable.

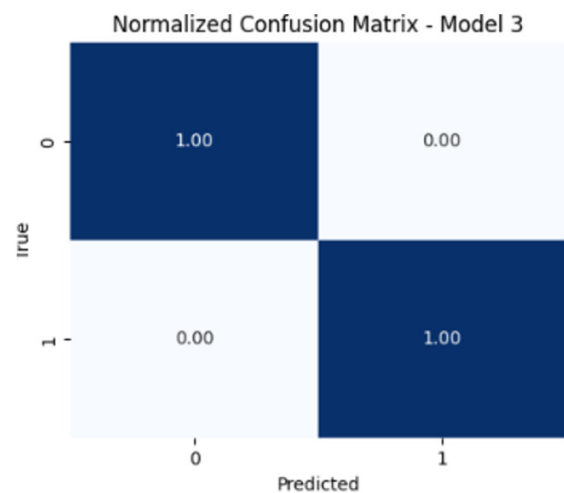


Fig. 10. Normalized confusion matrix of Model 3.

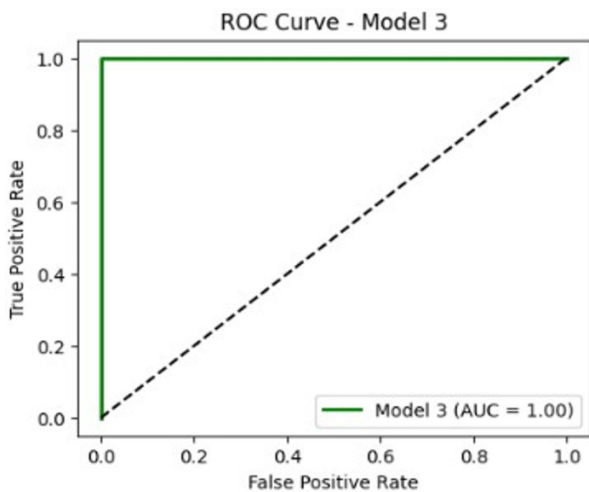


Fig. 11. ROC curve of Model 3 illustrating class separability (AUC = 1.0).

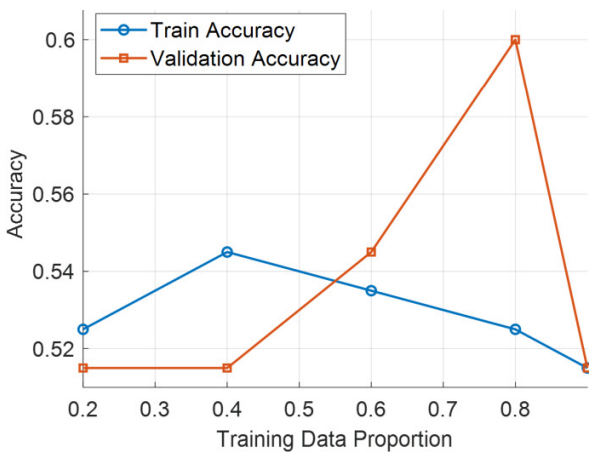


Fig. 12. Learning curve of the model for various training sets.



Fig. 13. Stability check of the model for 5 runs.

Similar trends were observed in the test accuracy, which shows moderate variation (mean 0.9520, std 0.0960, range 0.7601-1.0000), indicating that the model achieves a very good performance; however, some runs show a significant increase in accuracy. This behavior can be attributed to stochastic effects such as random initialization and mini-batch selection. The change in learning rate can be attributed to the Reduce LR On Plateau effect occurring in some runs. These trends suggest that convergence is dynamic, with all runs achieving high accuracy with small variation in individual runs.

Figure 14 illustrates the impact of Gaussian noise on the classification performance of Model 3, showing a noticeable reduction in accuracy as noise intensity increases. The results indicate that the presence of noise significantly affects accuracy, with performance decreasing as the noise level increases. With a low noise standard deviation of 0.01, the test accuracy decreases to 78.0%, indicating that even small disturbances could affect the predictions; however, the model performs reasonably well. When the noise is increased to 0.05, there is a steep decline in accuracy to around 52.0% (which is almost at random chance for a binary classification), with a significant increase in the test loss. These results indicate that the model is highly sensitive to even small signal perturbations. When the noise level was set to 0.1, the predictions became unreliable, with the model achieving only 50% prediction accuracy.

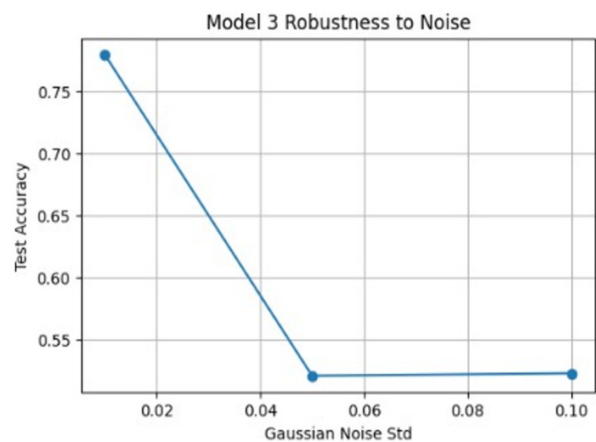


Fig. 14. Effect of Gaussian noise on the performance of Model 3.

## VI. CONCLUSION

This study evaluated A hybrid Convolutional Neural Network (CNN)–Long Short-Term Memory (LSTM) model, which integrates Electroencephalography (EEG) and Electromyography (EMG) signals to classify Parkinson's Disease (PD) patients from healthy controls. EEG signals were collected using a high-resolution, 14-channel wireless EEG headset, while EMG data were acquired from three sensors placed according to the SENIAM standard.

The results indicate that, compared to existing studies that rely on either EEG or EMG signals independently, the proposed work offers a more comprehensive representation of PD by integrating both neural and muscular information within a unified framework. Prior EEG-based approaches effectively capture cortical abnormalities but overlook peripheral motor manifestations, while EMG-only methods fail to reflect underlying neural dysfunction. Unlike earlier multimodal studies that primarily employ conventional machine learning classifiers such as Support Vector Machines (SVM) with handcrafted features, this work adopts a hybrid CNN–LSTM architecture that automatically learns spatial and temporal characteristics from raw EEG and EMG signals. Furthermore, most related works are limited to offline analysis, whereas the proposed system supports both offline and real-time prediction

using low-cost wearable hardware. This multimodal, deep learning-based, and real-time capable framework demonstrates superior classification performance, highlighting the novelty and practical contribution of the proposed approach for early PD detection.

#### DECLARATION OF COMPETING INTERESTS

The authors declare no competing interests.

#### ACKNOWLEDGEMENT

The authors would like to thank Dr. Sathish Kumar for the support and encouragement provided throughout the study. The authors extend gratitude to the Asia Pacific University for providing the resources and support necessary for this research, which enabled the acquisition of new learning methods and additional knowledge in the field.

#### DATA AVAILABILITY

The EEG and EMG data used in this study were collected from [15-21]. Additional EEG signal data were collected from the San Diego dataset [23] and UNM EEG dataset [24].

#### REFERENCES

- [1] M. A. Alsuwaiket, "Feature Extraction of EEG Signals for Seizure Detection Using Machine Learning Algorithms," *Engineering, Technology & Applied Science Research*, vol. 12, no. 5, pp. 9247–9251, Oct. 2022, <https://doi.org/10.48084/etasr.5208>.
- [2] H. M. Adem, A. W. Tessema, and G. L. Simegn, "Classification of Parkinson's Disease Using EMG Signals from Different Upper Limb Movements Based on Multiclass Support Vector Machine," *International Journal Bioautomation*, vol. 26, no. 1, pp. 109–125, Mar. 2022, <https://doi.org/10.7546/ijba.2022.26.1.000849>.
- [3] T. Ahmed and Md. K. Islam, "EMG Signal Classification for Detecting Neuromuscular Disorders," *Journal of Physics: Conference Series*, vol. 1921, no. 1, May 2021, Art. no. 012043, <https://doi.org/10.1088/1742-6596/1921/1/012043>.
- [4] M. Allahbakhshi, A. Sadri, and S. O. Shahdi, "Diagnosis of Parkinson's Disease Using EEG Signals and Machine Learning Techniques: A Comprehensive Study," arXiv, 2024, <https://doi.org/10.48550/ARXIV.2405.00741>.
- [5] N. K. Al-Qazzaz, A. A. Aldoori, A. K. Buniya, S. H. B. M. Ali, and S. A. Ahmad, "Transfer Learning and Hybrid Deep Convolutional Neural Networks Models for Autism Spectrum Disorder Classification from EEG Signals," *IEEE Access*, vol. 12, pp. 64510–64530, 2024, <https://doi.org/10.1109/ACCESS.2024.3396869>.
- [6] M. F. Anjum, "Parkinson's Disease Classification via EEG: All You Need is a Single Convolutional Layer." arXiv, 2024, <https://doi.org/10.48550/ARXIV.2408.10457>.
- [7] G. Averta *et al.*, "U-Limb: A Multi-Modal, Multi-Center Database on Arm Motion Control in Healthy and Post-Stroke Conditions," *GigaScience*, vol. 10, no. 6, Jun. 2021, Art. no. giab043, <https://doi.org/10.1093/gigascience/giab043>.
- [8] R. Collier, "WHO guidelines on ethical public health surveillance," *Canadian Medical Association Journal*, vol. 189, no. 29, pp. E977–E977, Jul. 2017, <https://doi.org/10.1503/cmaj.1095453>.
- [9] R. Dubey, M. Kumar, A. Upadhyay, and R. B. Pachori, "Automated Diagnosis of Muscle Diseases from EMG Signals Using Empirical Mode Decomposition Based Method," *Biomedical Signal Processing and Control*, vol. 71, Jan. 2022, Art. no. 103098, <https://doi.org/10.1016/j.bspc.2021.103098>.
- [10] K. Desai, "Parkinson's Disease Detection via Resting-State Electroencephalography Using Signal Processing and Machine Learning Techniques." arXiv, 2023, <https://doi.org/10.48550/ARXIV.2304.01214>.
- [11] F. Morandín-Ahuerma, "Ten UNESCO Recommendations on the Ethics of Artificial Intelligence." *Normative Principles for an Ethics of Artificial Intelligence*, pp. 86–94, Sep. 2023, <https://doi.org/10.31219/osf.io/csyux>.
- [12] C. Fricke, J. Alizadeh, N. Zakhary, T. B. Woost, M. Bogdan, and J. Classen, "Evaluation of Three Machine Learning Algorithms for the Automatic Classification of EMG Patterns in Gait Disorders," *Frontiers in Neurology*, vol. 12, May 2021, Art. no. 666458, <https://doi.org/10.3389/fneur.2021.666458>.
- [13] N. Hooda, R. Das, and N. Kumar, "Fusion of EEG and EMG Signals for Classification of Unilateral Foot Movements," *Biomedical Signal Processing and Control*, vol. 60, Jul. 2020, Art. no. 101990, <https://doi.org/10.1016/j.bspc.2020.101990>.
- [14] S. Jose *et al.*, "Robust Classification of Intramuscular EMG Signals to Aid the Diagnosis of Neuromuscular Disorders," *IEEE Open Journal of Engineering in Medicine and Biology*, vol. 1, pp. 235–242, 2020, <https://doi.org/10.1109/OJEMB.2020.3017130>.
- [15] A. Kurbatskaya, A. Jaramillo-Jimenez, J. F. Ochoa-Gomez, K. Brønning, and A. Fernandez-Quilez, "Machine Learning-Based Detection of Parkinson's Disease from Resting-State EEG: A Multi-Center Study." arXiv, 2023, <https://doi.org/10.48550/ARXIV.2303.01389>.
- [16] A. Lensky, "Central and Central-Parietal EEG Signatures of Parkinson's Disease." *Frontiers in Neuroscience*, Mar. 2025.
- [17] K. Li, B. Ao, X. Wu, Q. Wen, E. Ul Haq, and J. Yin, "Parkinson's Disease Detection and Classification Using EEG Based on Deep CNN-LSTM Model," *Biotechnology and Genetic Engineering Reviews*, vol. 40, no. 3, pp. 2577–2596, Nov. 2024, <https://doi.org/10.1080/02648725.2023.2200333>.
- [18] S. J. Mitin *et al.*, "Bi-Cephalic Self-Attended Model to Classify Parkinson's Disease Patients with Freezing of Gait," *European Journal of Neuroscience*, vol. 63, no. 4, Feb. 2026, Art. no. e70433, <https://doi.org/10.1111/ejn.70433>.
- [19] H. Uyanik, A. Sengur, M. Salvi, R. Tan, J. H. Tan, and U. R. Acharya, "Automated Detection of Neurological and Mental Health Disorders Using EEG Signals and Artificial Intelligence: A Systematic Review," *WIREs Data Mining and Knowledge Discovery*, vol. 15, no. 1, Mar. 2025, Art. no. e70002, <https://doi.org/10.1002/widm.70002>.
- [20] World Medical Association, "World Medical Association Declaration of Helsinki: Ethical Principles for Medical Research Involving Human Subjects," *JAMA*, vol. 310, no. 20, Nov. 2013, Art. no. 2191, <https://doi.org/10.1001/jama.2013.281053>.
- [21] Z. M. Yusoff, "The Malaysian Personal Data Protection Act 2010: A Legislation Note," *New Zealand Journal of Public and International Law*, vol. 9, no. 1, 2011.
- [22] D. S. Tan, H. Nisar, K. H. Yeap, V. Dakulagi, and M. Amin, "Lumbar Intervertebral Disc Detection and Classification with Novel Deep Learning Models," *Journal of King Saud University - Computer and Information Sciences*, vol. 36, no. 7, Sep. 2024, Art. no. 102148, <https://doi.org/10.1016/j.jksuci.2024.102148>.
- [23] A. P. Rockhill, Nicko Jackson, Jobi George, A. Aron, and N. C. Swann, "UC San Diego Resting State EEG Data from Patients with Parkinson's Disease." *Openneuro*, 2022, <https://doi.org/10.18112/OPENNEURO.DS002778.V1.0.5>.
- [24] M. F. Anjum, S. Dasgupta, R. Mudumbai, A. Singh, J. F. Cavanagh, and N. S. Narayanan, "Linear Predictive Coding Distinguishes Spectral EEG Features of Parkinson's Disease," *Parkinsonism & Related Disorders*, vol. 79, pp. 79–85, Oct. 2020, <https://doi.org/10.1016/j.parkreldis.2020.08.001>.